Quaternary Research 81 (2014) 452–463

Contents lists available at ScienceDirect

Quaternary Research

journal homepage: www.elsevier.com/locate/yqres

Late Quaternary fluvial terraces near the Daocheng Ice Cap, eastern Tibetan Plateau

Liubing Xu *, Shangzhe Zhou

Department of Geography, South China Normal University, Guangzhou 510631, China

ARTICLE INFO

Article history:
Received 19 February 2013
Available online 26 September 2013

Keywords:
Fluvial terrace
Glaciation
Tectonic uplift
Climate change
Haizi Shan
Eastern Tibetan Plateau

ABSTRACT

The timing of terrace formation relative to the glacial–interglacial cycle and what factors control that timing, such as changes in climate and/or uplift, are controversial. Here we present a study of the terraces along the Yazheku River using electron spin resonance (ESR) dating and analysis of the sedimentary characteristics in order to establish the timing of terrace formation and to assess the forcing mechanisms that have been proposed. The Yazheku River flows in glacial trough leading from the Haizi Shan, on the eastern Tibetan Plateau. The range was uplifted during the Quaternary and repeatedly glaciated by ice caps. The four highest major terraces (T5, T4, T3, and T2) are the result of both climatic and tectonic influences. Strath terraces T5–T2 were created during Haizi Shan glacial expansions during MIS 16, 12, 6 and 3–4, respectively. The major aggradation phases of the four terraces occurred during the deglaciations at the ends of MIS 16, 12, 6, and 2. Down-cutting, which led to the generation of the four terraces, immediately followed the deposition of the T5–T2 gravel units. These incisions occurred during the transitions between MIS 16–15, MIS 12–11, MIS 6–5, and MIS 2–1.

Introduction

River terraces are landforms that were at one time constructed and maintained as the active valley floor of a river but are now abandoned. Creation of a fluvial terrace typically includes strath (also called 'bench' or 'bedrock surface' in some literature) cutting and sediment deposition, followed by river incision. The timing of these three processes is controversial (Penck and Brückner, 1909; Zeuner, 1945; Fisk, 1951; Bridgland, 2000; Hsieh and Knuepfer, 2001; Maddy et al., 2001; Pan et al., 2003; Vandenberghe, 2003; Cunha et al., 2005; Litchfield and Berryman, 2005; Pan et al., 2007). Penck and Brückner (1909) suggested that terrace deposits were the results of glaciations and their outwash, whereas the downcutting to generate the terraces took place during interglaciations. Fisk (1951) interpreted aggradation as a warm-climate phenomenon and considered incision to occur during glacial periods. In models of terrace formation along the River Thames (Bridgland, 2000; Maddy et al., 2001), vertical incision occurs during the transitions from glacial to interglacial climates while aggradation has been attributed to periods of cold climate, especially those during which the landscape (valley sides and slopes) was destabilized. More recently, Pan et al. (2003) stated that the straths in the Qilian Mountains of western China were abandoned during glacial-to-interglacial transitions. The timings of river aggradation and incision remain open questions, as does what influences are the most important to terrace formation. The answer may vary with rivers in different regions, and even along the different reaches of the same river. Our greatest opportunity of resolving these issues lies with chronological studies, because only precise and accurate ages can define the timing of terrace formation relative to the glacial–interglacial climate record and facilitate correlations to documented climatic and tectonic events (Pan et al., 2003).

Although the dating of landforms is critical to understand landscape evolution, reliable dates are often hard to obtain due to the lack of suitable dating materials and the limitations of various techniques. The recently developed cosmogenic nuclide dating method, for instance, is now widely used to constrain the ages of fluvial terraces; however, the accumulation history of cosmogenic nuclides in terrace sediments may be difficult to constrain due to the deposition and removal of overlying loess, and the removal of upper layers of terrace sediments, which are concerns in this study area. Although radiocarbon and luminescence dating are widely applied to constrain the chronologies of river terraces, the application of these techniques is limited to relatively recent landforms, as ^{14}C has a dating limit of ~40 ka, and luminescence dating of ~120 ka (Prescott and Robertson, 1997; Watchman and Twidale, 2002; Pan et al., 2007). Electron spin resonance (ESR) dating, however, offers the possibility of extending the time range of sediment dating to 1 Ma (Laurent et al., 1998; Pan et al., 2007). In this study we investigate the glaciofluvial terraces and the associated moraines of the Haizi Shan in the central Hengduan Mountains of the eastern Tibetan Plateau (Figs. 1 and 2). According to the results of ESR dating, in association with morphostratigraphic analysis, we have developed a new chronology of the terraces. Based on the ages, we assess the impacts of tectonic activity, climatic change, and glaciations in the Haizi Shan on the formation of these glaciofluvial terraces.

* Corresponding author. Fax: +86 20 85215910.
E-mail address: xuliubing234@163.com (L. Xu).

0033-5894/$ – see front matter © 2013 University of Washington. Published by Elsevier Inc. All rights reserved.
http://dx.doi.org/10.1016/j.yqres.2013.08.007

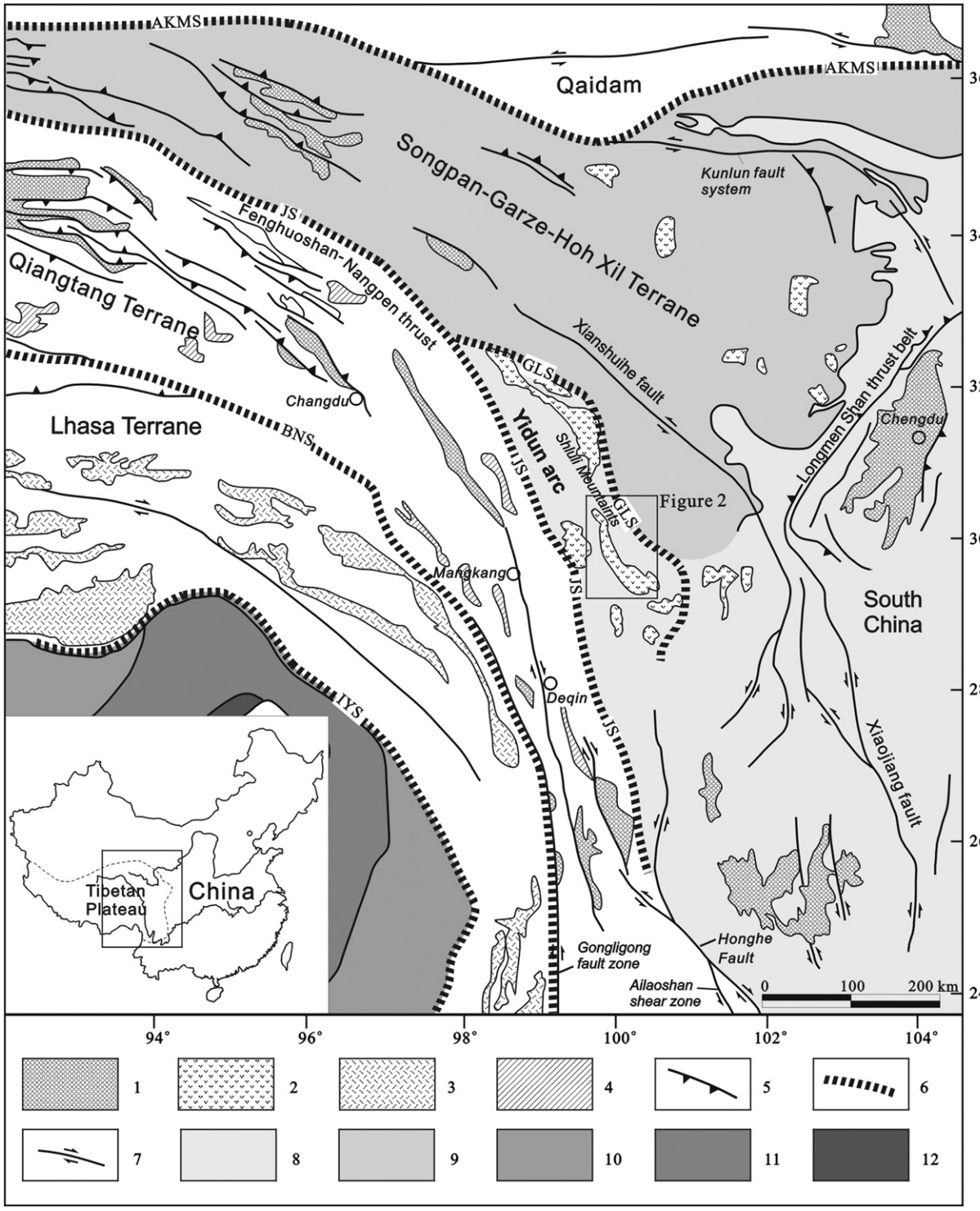

Figure 1. Simplified tectonic map of the Hengduan Mountains, modified from Hou et al. (2004). In the square is the Haizi Shan, as presented in Fig. 2. AKMS—Animaqing–Kunlun–Muzitage suture zone; JS—Jinshajiang suture zone; GLS—Ganze–Litang (or Yalongjiang) suture zone; BNS—Bangongcuo–Nujiang suture zone; IYS—Indian River–Yaluzangbo suture zone; 1—Tertiary sedimentary rocks; 2—Miocene plutons in Songpan–Ganze terrane; 3—Late Triassic plutons in Yidun arc; 4—Miocene plutons in Qiangtang terrane; 5—thrust fault; 6—suture zone; 7—strike-slip fault; 8—Yangzi plate; 9—Songpan–Ganze terrane; 10—Tethyan-Himalaya; 11—High-Himalaya; 12—Low-Himalaya.

Geologic and climatic setting

The Yazheku River, a third-order tributary of the Yangtze, originates from the Haizi Shan in the central Shaluli Mountains, southeastern Tibetan Plateau (Fig. 2). The Shaluli Mountains, stretching ~450 km in a south–north direction and with an average altitude of ~4500 m asl (above sea level), are the widest range of the Hengduan Mountains. Tectonically, the Shaluli Mountains form the main part of the Yidun arc orogen, which extends approximately in an N–S direction for ~500 km between the Jinshajiang and Ganze–Litang (or Yalongjiang) Rifts (Fig. 1). The formation and evolution history of the Yidun arc can be summarized as follows: (1) A large-scale Indosinian subduction–orogenesis led to the formation of the Yidun magmatic arc (238–210 Ma); (2) Following ~206 Ma there occurred an arc-continent collision accompanied by transpressional deformation of the arc crust; (3) In the late Yanshanian epoch (138–73 Ma) post-orogenic extension resulted in

https://doi.org/10.1016/j.yqres.2013.08.007 Published online by Cambridge University Press

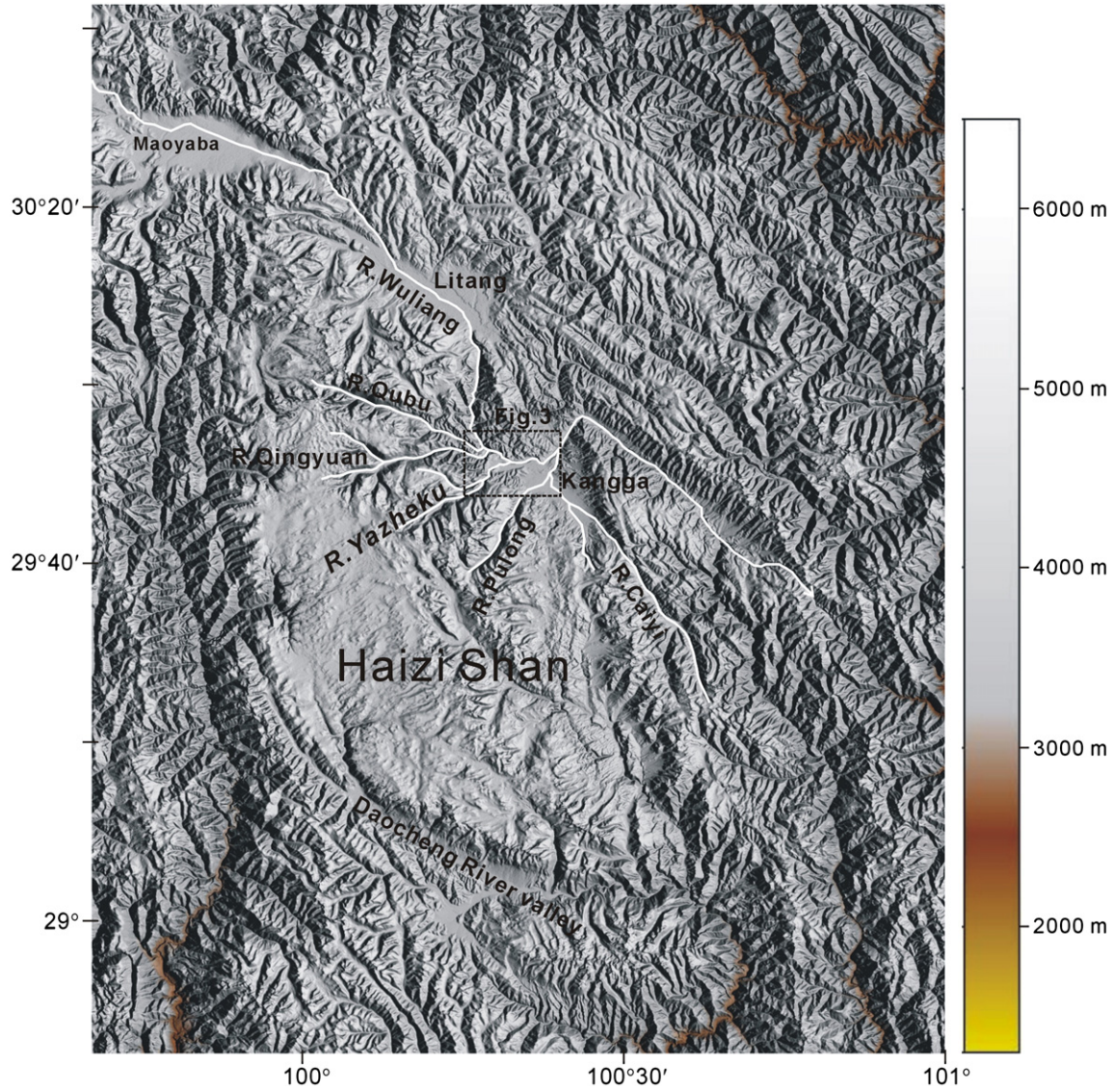

Figure 2. Digital shaded-relief image showing the location of the Yazheku River and its relation to the Haizi Shan, and other main river valleys originating from the Haizi Shan as well. The square indicates the area of Fig. 3 in which a distribution of terraces along the Yazheku and Wuliang Rivers is presented.

the generation of A-type granites; and (4) During the Himalayan period (65–15 Ma) intra-continental orogenic movement prevailed and was accompanied by large-scale strike-slip thrusting, resulting in the intrusion of granites and development of pull-apart basins (e.g., the Maoyaba, Litang, and Kangga basins as shown in Fig. 2) (Hou et al., 2001, 2004). These basins contain Neogene red clay beds that are tens of meters thick. These are deeply weathered soils that certainly did not form under modern climatic conditions (i.e., with an altitude of ~4000 m; mean annual temperature 3.1°C; mean temperature in July 10.2°C; mean annual precipitation ~700 mm) in this region. It is likely that they were generated at a much lower altitude and then uplifted to the current elevation. Shi et al. (1995) inferred an uplift amplitude of over 1000 m since the end of the Neogene. Vertical uplift dominated during the late Cenozoic in the Tibetan Plateau (including the Shaluli Mountains in the eastern Plateau). The main late Cenozoic uplift events can be generalized as: (1) the Qingzang Movement from 3.6 to 1.7 Ma; (2) the Kunlun–Huanghe Movement during ~1.2–0.6 Ma; and (3) the Gonghe Movement at ~0.15 Ma (e.g., Li et al., 1996; Cui et al., 1997, 1998; Li and Fang, 1998). A great number of relics (with different ages) of the Quaternary faulting activities have been found in the Haizi Shan and its vicinity, which indicates that the crust in this region was unstable during the Quaternary (Xu et al., 2005). Repeated leveling measurements carried out by Zhang et al. (1990) show that the modern Tibetan Plateau is still actively being uplifted at an average rate of 5.8 mm/yr.

The Shaluli Mountains have been repeatedly glaciated since the middle Pleistocene (Zheng and Ma, 1995; Li, 1996; Xu and Zhou, 2009). Ice caps with areas of thousands of square kilometers and thicknesses of up to hundreds of meters have repeatedly developed in the Haizi Shan during the Quaternary (Zheng and Ma, 1995; Li, 1996). Based on geomorphic evidence and ESR ages of glacial and glaciofluvial sediments, Xu and Zhou (2009) identified six major glacial advances during the middle and late Pleistocene. These glacial expansions have been assigned to marine oxygen isotope stages (MIS) 16, MIS 12, MIS 6, MIS 3, and the Last Glacial Maximum (LGM). Wang et al. (2006) also recognized three glacier advances corresponding to MIS 16, MIS 6, and the LGM, on the basis of cosmogenic radionuclide ^{10}Be dating.

Climatically, the Shaluli Mountains are dominated by the south Asian monsoon in the summer and the mid-latitude westerlies in the winter (Lin and Wu, 1990; Shi, 2006). The westerlies, however, contribute little precipitation to this region, because the moisture carried by them from the Atlantic Ocean and Mediterranean Sea decreases sharply from west to east across the Tibetan Plateau and very little moisture

https://doi.org/10.1016/j.yqres.2013.08.007 Published online by Cambridge University Press

remains when the air masses reach the Shaluli Mountains (Li, 1996; Shi, 2002, 2006). In summer, the moisture from the Indian Ocean and Bay of Bengal is transported by the south Asian monsoon into the Hengduan Mountains via the deep-incised river valleys (e.g., the Yarlung Zangbo, Jinshajiang, Lancangjiang, Yalongjiang Rivers) of the southeastern Tibetan Plateau (Lin and Wu, 1990; Zheng et al., 1997; Zhuo et al., 2002). Most of the precipitation in the Shaluli Mountains is delivered by the summer Asian monsoon (Shi, 2006). Statistical data presented by Shi (2006) show that the precipitation during the warmer half of the year (May–October) accounts for 89–96% of the average annual total in the Hengduan Mountains, and 91% in the Shaluli Mountains. Moreover, precipitation increases with altitude. For example, in the Litang Basin (~3730 m asl; ~15 km northeast to the Yazheku drainage basin) it is 720 mm and increases to ~1150 near the snow line (5100–5150 m asl), an increase of 60% (Shi, 2006).

Terrace records in the Yazheku River

Four glacial troughs, currently called the Qubu, Qingyuanku, Yazheku and Pulongqu Valleys, originate from the northeastern part of the Haizi Shan and eventually join the valley of the Wuliang River (Figs. 2 and 3). In its trough the Yazheku River flows northeastward for about 19 km to the Wuliang. A flight of five major fluvial terraces (we refer to them as T1, T2, T3, T4, and T5 from younger to older) and three minor (fill-and-cut) terraces (T2a, T2b, and T2c, from young to old) can be identified along the lower 2 km of the Yazheku (immediately above its confluence with the Wuliang) (Fig. 3). Two kilometers upstream from the confluence, the river valley becomes a narrow gorge, with strath terraces absent or rarely present and a bedrock floor. All the five major and three minor terrace units are described here, but we are especially interested in the four higher terraces (T2–T5) because they have a close relationship to the Quaternary glaciations in the Haizi Shan.

The first terrace level, T1, is a typical fill terrace only present on the southern side of the Yazheku River (Figs. 3 and 4). The tread of T1 is ~9 m above the modern river level (arl). At the confluence of the two rivers, T1 joins with the first terrace of the Wuliang and is almost continuous downstream until it terminates 1 km east of Runiao, having a total length of ~12 km (Fig. 3). The T1 fills consist of multiple gravel–sand units, which are overlain by overbank deposits (mainly consisting of silt and fine sand) approximately 50 cm in thickness. The gravel clasts of T1 have a much lower sphericity than those of the first terrace of the Wuliang, probably partly because of a shorter transportation distance.

The second terrace T2 is well-preserved on both sides of the Yazheku (Fig. 3). The southern edge of T2 combines with the second terrace of the Wuliang at the confluence of the Yazheku and Wuliang rivers and extends continuously eastward, then turns northeastwards approximately at Kangga and eventually terminates near Runiao (Fig. 3). It has a total length of ~10.5 km. This second terrace is also (but discontinuously) preserved along the north side of the Wuliang River. Moreover, interfluves (marked as T2? in the lower-right corner of Fig. 3) in the Kangga Basin were probably deposited during the same period as the T2 sediments. Several small-scale landslides or collapses have occurred along the outer margins of T2 (Fig. 3). These are likely to have been caused by lateral erosion of the ancient or modern river channel. The tread of T2 rises ~90 m above the modern river level and is locally up to ~1500 m wide. The Triassic sandy slate strath is overlaid by ~3–4 m of gravel capped by ~2 m of coarse-sized sand, which is in turn covered by ~100–150 cm-thick loess. Abundant boulders, ranging from several decimeters up to ~3 m in diameter, are present in the gravel. In particular, several granite boulders crop out of the overlying sand and loess layers.

Along the outer side of the southern edge of T2 are several small discontinuous terraces (Figs. 3 and 4). They are fill-and-cut terraces and share the same strath with T2. These small terraces were likely formed by cutting into the T2 sediments through Bull's (cf. Bull, 1990, 1991) 'complex response' of the Yazheku and Wuliang Rivers. Four samples (YZKT301, YZKT302, YZK01, and YZK02) for ESR dating were collected from the silt- to sand-sized fraction within the gravel units of T2.

T3, ~120 m arl is present only on the northern side of the Yazheku (Figs. 3 and 4). The tread, ~100–600 m wide, is overlain by ~180 cm-thick loess. The strath is covered by ~4 m of gravel overlain by ~1.5 m of coarse-sized sand. The gravel contains abundant boulders with the largest reaching 3 m in diameter and some showing 2–3 cm thick weathering rinds. Similar to T2, many boulders are scattered in the loess deposits, but are actually protruding from the underlying gravel

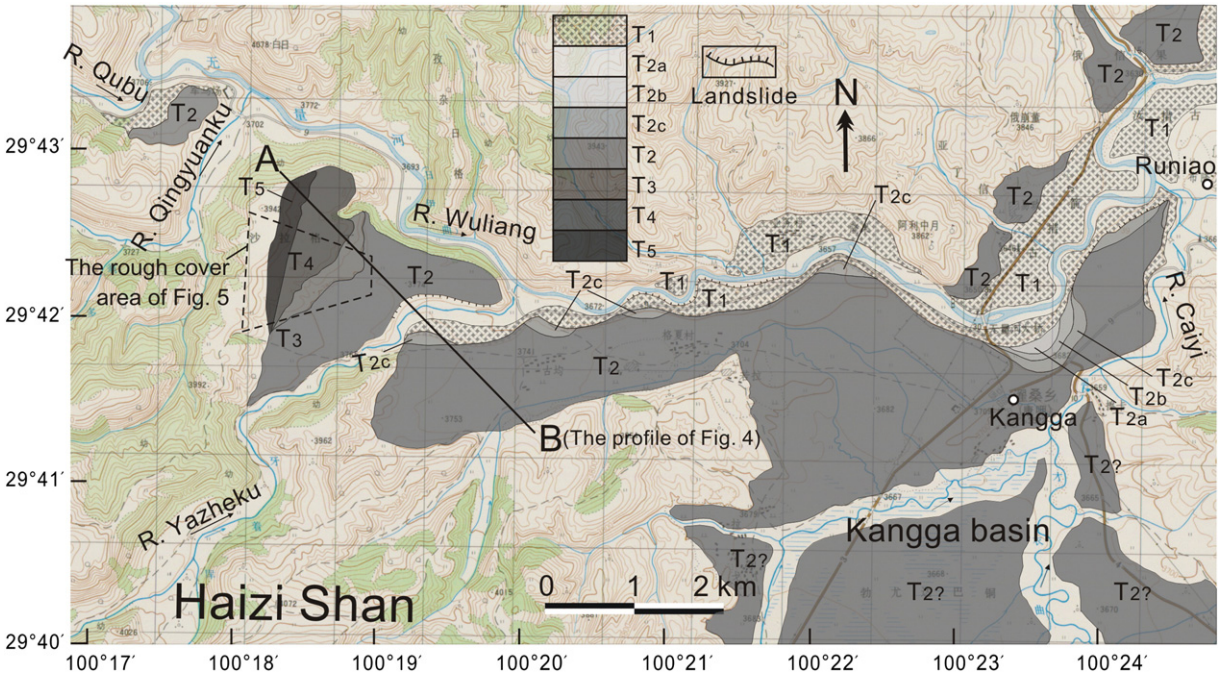

Figure 3. Distribution of the terraces in the lower reach of the Yazheku River. Moreover, the distribution of terraces along the Wuliang River is also presented to show their correlation with the Yazheku River terraces. A–B refers to the cross-valley profile as shown in Fig. 4.

https://doi.org/10.1016/j.yqres.2013.08.007 Published online by Cambridge University Press

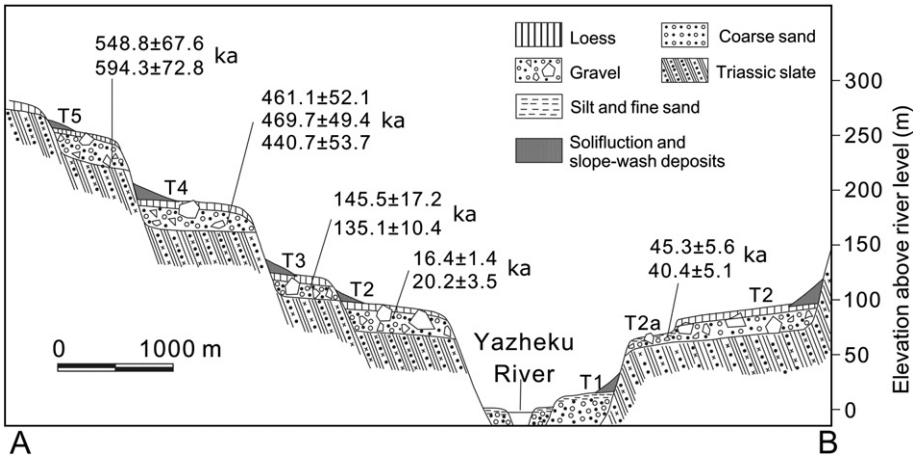

Figure 4. Cross-valley profile ("A–B" shown in Fig. 3) showing the stratigraphic relationship of terraces in the lower reach of the Yazheku River, sampling locations, and ESR ages (with the unit of ka) as well.

layer. In the middle part of T3, a few gullies of up to several meters in depth have been cut and the outer margin of the terrace exhibits a gentle slope (Fig. 5), indicating that the terrace has undergone substantial erosion. The material eroded from T3 was deposited along the inner edge of terrace T2 (Fig. 5). For the same reason, the loess layer on the inner edge of the T3 tread is mostly mantled by slope-wash and solifluction deposits from the upper terrace (i.e., T4), which are up to ~15 m thick. Two ESR samples (YZKT401 and YZK03) were collected from the fine sand fraction within the gravel.

T4 exists only on the northern side of the river (Figs. 3 and 4). The tread, ranging from ~100 m to ~500 m wide, stands ~160–180 m above the modern river level and is mantled by ~180 cm-thick loess. The strath is covered by ~2 m of gravel overlain by 1 m of sand. The gravel has a lower frequency of boulders and the grain size of the boulders is relatively small when compared with T2 and T3. A sediment exposure excavated by local shepherds revealed the clasts of T4 to be more highly weathered than those of T3. For example, weathering rinds of up to ~6–8 cm can be seen on some boulders. The southern part of the terrace tread has been dissected by gullies into numerous flat-topped small landforms (Figs. 3 and 5). The outer edge of the northern part is also dissected by gullies and has a gentle slope. The inner side of the T4 tread is in places capped by more than ten meters of solifluction and slope-wash deposits from the upper terrace T5. Fine sand within the gravel was sampled (YZKT502, YZKT503, and YZK04) for ESR dating.

The highest terrace, T5, is preserved only on the northern side of the Yazheku River (Figs. 3 and 4). The tread, ~230–250 m arl is ~100–200 m wide and overlain by 220-cm-thick loess. Numerous gullies have cut into the southern part of the tread; in contrast, the northern part of T5 is well preserved. The Triassic sandy slate strath is mantled by a ~3-m-thick layer of gravel covered by a ~1–2 m of coarse-sized sand. Boulders within the gravel are deeply weathered. A 30–50 cm-thick weathering rind is present on some large granitic boulders while most relatively small boulders have been weathered into white kaolinite. In between the boulders are deeply weathered silt and sand. ESR samples YZKT602 and YZK05 were collected from the fine sand-sized fraction within the gravel.

Methods

Sediment samples for dating by electron spin resonance (ESR) were collected from artificially exposed sections >1 m deep without exposure to sunlight. Silt- to sand-sized sediments were sampled from fluvial deposits. Samples were only collected from locations where the immediate surrounding sediment (>30 cm radius) was homogenous. The latitude, longitude and altitude of the samples were determined using handheld GPS devices. The samples were kept in opaque bags until processed at the Lanzhou University Chronology Laboratory.

The germanium (Ge) center was used as the ESR dating signal in this work. Although the Ge center is one of the most light-sensitive centers in quartz (Rick, 1997; Toyoda et al., 2000), its exposure to normal laboratory light does not affect the signal intensity (Walther and Zilles, 1994). The absorption band of the Ge center is ~4.43 eV, corresponding to a wavelength of 280 nm (Jin et al., 1991), which is beyond natural room light band, but lies within UV light band. Schwarcz (1994) suggested that samples with the Ge signal to be measured could be prepared in normal laboratory light. In this study, all samples were treated

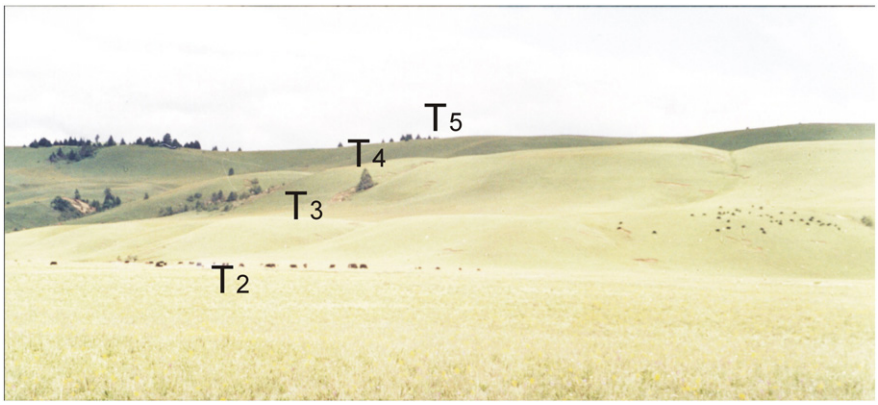

Figure 5. A picture showing the geomorphic features (e.g., gullies, solifluction and slope-wash deposits, as well as gental slope of the frontal margins of the treads) of terraces T2–T5 on the north side of the lower Yazheku River.

https://doi.org/10.1016/j.yqres.2013.08.007 Published online by Cambridge University Press

under normal laboratory light conditions, without special measurements being undertaken.

Sample preparation was carried out in the MOE Key Laboratory of Western China's Environmental System, Lanzhou University, according to the procedures described by Zhao et al. (2006, 2010) and Xu and Zhou (2009). Each sample was divided into two parts. A small fraction (~50 g) of each sample was dried in an oven at 40°C to estimate the in situ water content and then ground in an agate mortar and sieved through a 0.05 mm mesh. This part was then used to determine the concentrations of radioactive elements (U, Th, and K). The other fraction was washed in purified water to remove unbound clay and silt, and then sieved to obtain the 90–150 μm particle size fraction, which was treated with H_2O_2 to remove organic material. The grains were then soaked in 6 N HCl for 2 weeks to dissolve carbonate. The samples were soaked in 45% HF for ~2 h to etch the outer layers of the quartz grains, which are commonly damaged by alpha rays. The samples were thoroughly washed and dried at 40°C. Magnetic minerals were removed using a magnetic separator.

Purified quartz (~98%) from each sample was divided into nine aliquots (~250 mg each) and irradiated, with an artificial ^{60}Co-source with different doses, at the Institute of High Energy Physics, Chinese Academy of Sciences. The irradiating doses were monitored with alanine/ESR dosimeters. Some short-lived elements (e.g., Li, Na, and K) probably could be produced during artificial irradiation and they could affect the Ge signal at g = 1.997. To remove the signals of the potentially produced short-lived elements, the irradiated samples had been stored for three months before ESR measurement. The samples were measured using an ECS106-ESR spectrometer at the ESR Dating Laboratory, Qingdao Institute of Marine Geology, Ministry of Geology and Mineral Resources. The measurement conditions at room temperature were: X-band; microwave power—2 mW; modulation amplitude—0.1 mT; central magnetic field—348 ± 2.5 mT; sweep width—5 mT; change time—5.12 mS; time constant—40.96 mS; and amplification—1×10^5. To improve the signal/noise ratio, each sample was measured three times under the same measuring conditions. Figure 6 shows the natural and irradiated ESR spectra of quartz samples from terrace sediments of different stratigraphic ages.

The concentrations of U, Th, and K for calculating annual dose rates (D) were measured by laser fluorescence, colorimetric spectrophotometry, and atomic absorption, respectively. In dose rate calculations, conversion factors from Adamiec and Aitken (1998) were used; attenuation factors are from Mejdahl (1979) and the water absorption correction is from Grün (1989). The formula of Prescott and Hutton (1994) for a sample density of 2.3 g/cm^3 was utilized to calculate the cosmic dose rate. As the concentration of radioactive elements in quartz was below the range of measurement, the internal dose contributions were not taken into account in the dose rate determination. The contributions of α-radiation were excluded because the surface layers of the quartz grain had been removed by HF. Least-squares analysis was used to fit the data points based on the different artificial irradiation doses and the corresponding signal intensities. A linear fitting method was used in this work. The curve was then extrapolated to zero and to obtain the total dose (TD). Figure 7 shows an example of fitting line between artificial radiation doses and ESR signal intensity. Finally, ESR ages were calculated using the equation, T = TD / D.

Results

ESR dating results are shown in Table 1. The terrace sediments of T5–T2 were dated to 548.8 ± 67.6–594.3 ± 72.8 ka, 440.7 ± 53.7–469.7 ± 49.4 ka, 135.1 ± 10.4–145.5 ± 17.2 ka and 16.4 ± 1.4–45.3 ± 5.6 ka, respectively. All ages are consistent with stratigraphic order as described above. These age groups can be approximately assigned to MIS 16–14, 12, 6, and 3–2, respectively. It is interesting to note here that we have identified six lateral moraine ridges (here we refer to them, from the old to young, as M6–M1) in the Daocheng River valley, near the southern margin of the Haizi Shan (cf. Xu and Zhou, 2009). These six moraine ridges have been demonstrated to have been formed by Haizi Shan glacial advances during MIS 16 (M6), 12 (M5), 6 (M4), 3 (M3), and 2 (M2 and M1). In the following sections,

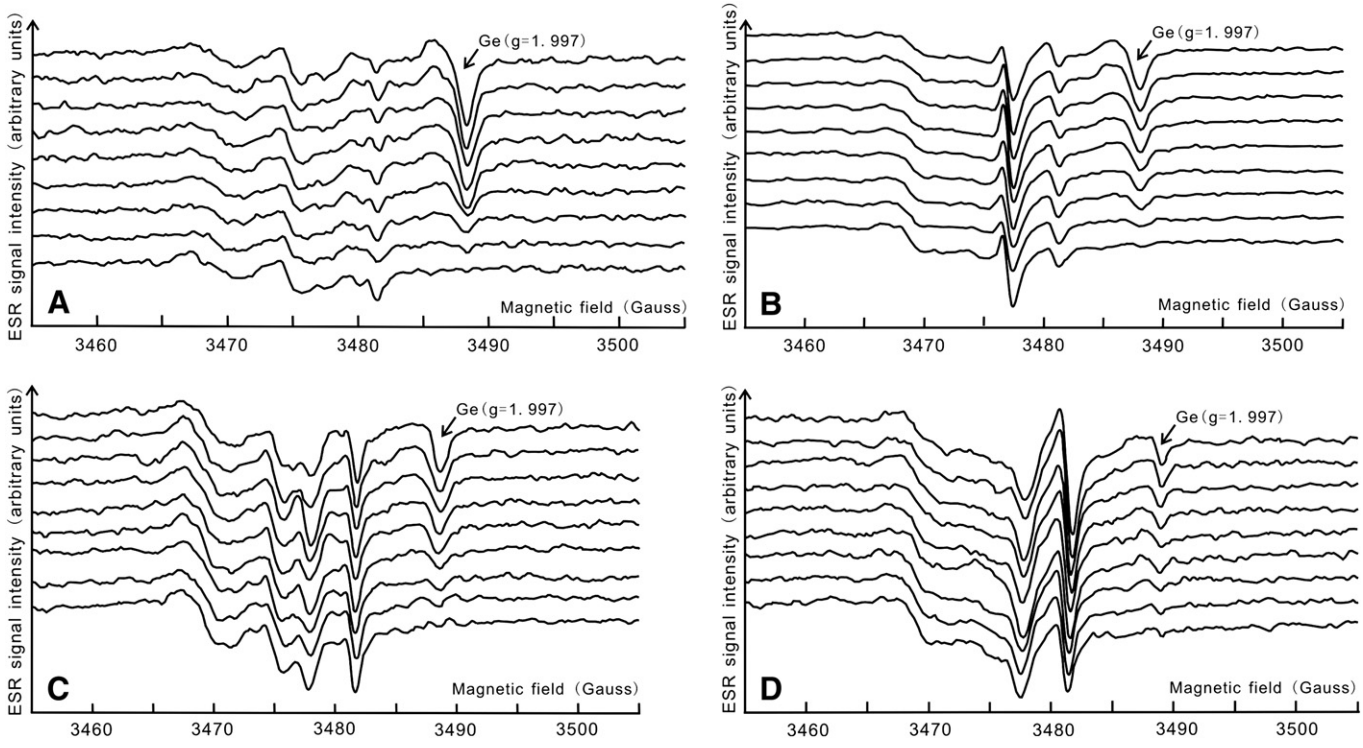

Figure 6. The natural and irradiated ESR spectra of quartz samples from terraces of different stratigraphic ages. (A) YZK02 (collected from terrace T2), (B) YZK03 (T3), (C) YZK04 (T4), and (D) YZK05 (from T5).

https://doi.org/10.1016/j.yqres.2013.08.007 Published online by Cambridge University Press

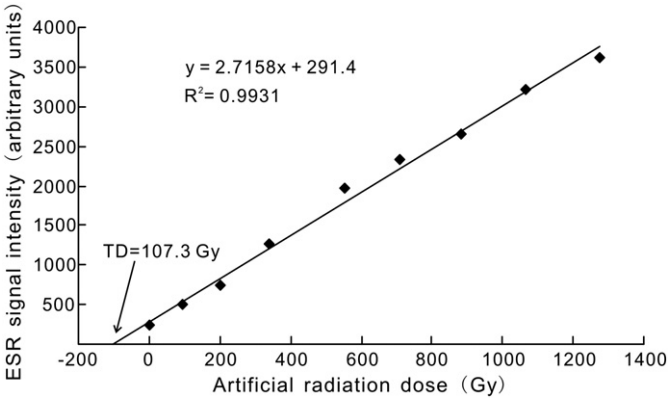

Figure 7. Dose response curve of ESR intensity of sample YZK02 collected from T2.

we will discuss in detail the formation mechanisms and processes of terraces T5–T2 in the Yazheku River according to the ESR ages and the relationships between the terraces and glacial expansions.

Discussion

Factors affecting the formation of Yazheku river terraces

Factors affecting the formation of river terraces can be summarized as intrinsic (internal fluvial system dynamical changes) and extrinsic (changes in external variables such as climate, tectonics, or base level) mechanisms (Bull, 1990, 1991; Maddy et al., 2001). We can be confident that intrinsic causes are not the primary cause for the formation of the Yazheku River terraces, except for T2a, T2b, and T2c, because the impact of intrinsic changes is limited both temporally (10–1000 yr) and spatially (at 10–1000 m scale) (Maddy et al., 2001). Moreover, the Yazheku River is far beyond the influence of cyclic sea-level variations, as the river is thousands of meters above the modern sea level.

Changes in local base level also cannot be used to explain terrace formation in the Yazheku River. Although the Kangga basin, ~3 km east to the Yazheku River, was once a lake with a limited area of ~9 km^2, the paleo-lake disappeared ~800 ka due to tectonic uplift in this region (Li, 1996). The existence of the lake pre-dates the oldest terrace (T5) with an age of less than 700 ka. Moreover, for terraces resulting from changes of base level, terrace surfaces typically show a convergent trend upstream (Wegmann and Pazzaglia, 2002), which contrasts with the divergence upstream of the Yazheku terraces.

The Quaternary climate was characterized by rhythmic fluctuations, which have played an important role during terrace formation via cyclically impacting on the regional hydrological regime and sediment load (Starkel, 2003). Numerous models (e.g., Penck and Brückner, 1909; Fisk, 1951; Bridgland, 2000; Maddy et al., 2001; Pan et al., 2007) for terrace formation under the influence of Quaternary cyclic climatic fluctuation have been proposed. Although climate-driven changes are undoubtedly important in controlling aggradation–incision cycles, climatic forcing alone is insufficient to cause river terrace staircases to form, because climate fluctuations during the Quaternary have been largely cyclic (Maddy, 1997; Bridgland, 2000; Maddy et al., 2001). The tendency of progressive channel incision during the Quaternary, which has led to the formation of terrace staircases, suggests that another mechanism is required (Maddy, 1997; Bridgland, 2000; Maddy et al., 2001). Tectonic forcing on terrace formation has been widely reported throughout the world (e.g., Pazzaglia and Brandon, 2001; Wegmann and Pazzaglia, 2002; Westaway et al., 2002; Demir et al., 2004; Pan et al., 2007). Additionally, isostatic uplift (i.e., isostatic crustal rebound), resulting from glacier melting (glacio-isostasy) and/or from erosion (erosional isostasy), has been found to be a critical forcing in terrace formation (e.g., Bridgland, 2000; Maddy and Bridgland, 2000; Bridgland et al., 2010).

As cited above ("Geologic and climatic setting"), the Haizi Shan region has been uplifted during the Quaternary, probably >1000 m. In the following section, the formation process of the terraces in the Yazheku River will be discussed, in the context of tectonic uplift and cyclic climate fluctuations during the Quaternary.

Terrace formation along the Yazheku River

Boulders in the sediments of terraces T5–T2

As presented above, five major terraces are present in the lower reach of the Yazheku River. Except for T1, T2a, T2b, and T2c, which are fill or fill-and-cut terraces, all are strath terraces. The width of terrace treads is typically hundreds of meters, with the broadest tread (T2) reaching 1500 m. Each of the terrace sediments of T5–T2 is characterized by a two-unit structure, i.e., a 2–4 m thick gravel overlaid by a 1–2 m thick sand layer. The terrace sediments are then overlain by ~1–2 m of loess, itself partly mantled by solifluction and slope-wash deposits with depths of several to >10 m.

It is interesting to note that the gravel units of T5–T2 contain numerous boulders with diameters varying from tens of centimeters to several meters. Over 90% of the boulders is granite, although the bedrock beneath the terraces is Triassic sandy slate. Granite bedrock is distributed on the planation surface of the Haizi Shan. The most reasonable explanation for the origin of the boulders is that they were glacially sourced. In regard to boulder transportation, there are three possibilities, i.e., by glacial, fluvial, or glaciofluvial processes. Direct transport by glaciers can be excluded, otherwise the terraces would have been destroyed. Pure fluvial transport of these boulders could only occur during full interglacial conditions, when glaciers in the drainage area of the Yazheku should have greatly reduced or even eliminated. The drainage basin, however, has an area of only ~42 km^2 (with mean annual precipitation of ~700 mm). Thus, it seems unreasonable for such a small-scale

Table 1
Summary of dating results by ESR from 90–150 μm quartz extracted from sediment matrix: sample locations, radionuclide concentrations, in situ water contents, cosmic dose rates, total dose rates, total dose estimates (TD) and ESR ages.

Sample no	Sampling site	Latitude (°N)	Longitude (°E)	Depth (m)	Altitude (m asl)	$W_{in\ situ}$ (%)	U (ppm)	Th (ppm)	K_2O (%)	Cosmic (mGya^{-1})	Total dose-rate (mGya^{-1})	TD (Gy)	Age (ka)
YZKT301	T2	29°41.81′	100°19.42′	1.7	3769	6.24	4.53	17.8	2.94	0.283	5.18	209.4	40.4 ± 5.1
YZKT302	T2	29°41.84′	100°19.67′	1.4	3770	6.19	4.67	18.1	3.21	0.296	5.48	248.2	45.3 ± 5.6
YZK01[a]	T2	29°42.38′	100°19.83′	5.6	3772	1.83	4.98	17.9	3.43	0.163	5.86	118.6	20.2 ± 3.5
YZK02[a]	T2	29°42.3′	100°19.53′	5.9	3774	4.48	2.39	18.2	2.98	0.157	5.31	107.3	16.4 ± 1.4
YZK03[a]	T3	29°42′	100°18.53′	4.5	3801	5.41	4.39	20.0	3.81	0.190	6.01	810.8	135.1 ± 10.4
YZKT401	T3	29°41.78′	100°18.5′	4.7	3803	5.13	4.02	18.5	3.05	0.185	5.17	751.5	145.5 ± 17.2
YZK04[a]	T4	29°42.37′	100°18.49′	5.8	3860	5.26	5.03	17.6	2.77	0.161	5.08	2388.1	469.7 ± 49.4
YZKT502	T4	29°42.25′	100°18.31′	5.2	3862	4.78	4.53	21.2	2.71	0.175	5.22	2405.1	461.1 ± 52.1
YZKT503	T4	29°42.41′	100°18.72′	5.6	3859	5.24	5.14	19.7	2.88	0.166	5.37	2365.5	440.7 ± 53.7
YZK05[a]	T5	29°41.88′	100°17.58′	6.7	3955	5.17	4.47	18.9	3.65	0.146	5.78	3171.8	548.8 ± 67.6
YZKT602	T5	29°42.28′	100°18.10′	6.4	3956	4.98	4.72	17.6	3.71	0.152	5.16	3064.7	594.3 ± 72.8

[a] Cited from Xu and Zhou (2009).

https://doi.org/10.1016/j.yqres.2013.08.007 Published online by Cambridge University Press

drainage basin to produce enough hydro-kinetic power to transport these boulders to their positions in terraces T5–T2. Thus the boulders were presumably transported downstream to terraces T5–T2 by glaciofluvial discharge, likely with the help of floating ice. The timing of these transport processes requires consideration. Two prerequisites should be met during the transport processes, i.e., the necessary conditions for the supply of these boulders, and sufficient (glacio)-fluvial discharge for transporting them, especially the largest ones.

During glacial periods, precipitation is thought to have decreased due to the weakened south Asian monsoon then (Fig. 8). Furthermore, precipitation occurred mainly as snow at high altitudes in association with low temperatures, resulting in glacier advance in the Haizi Shan. During glacier movement, large numbers of clasts of different sizes (including boulders) were excavated and frozen into the glaciers. At times of glacial expansion, extensive permafrost and seasonal frost would have formed in response to the low temperature. As a result,

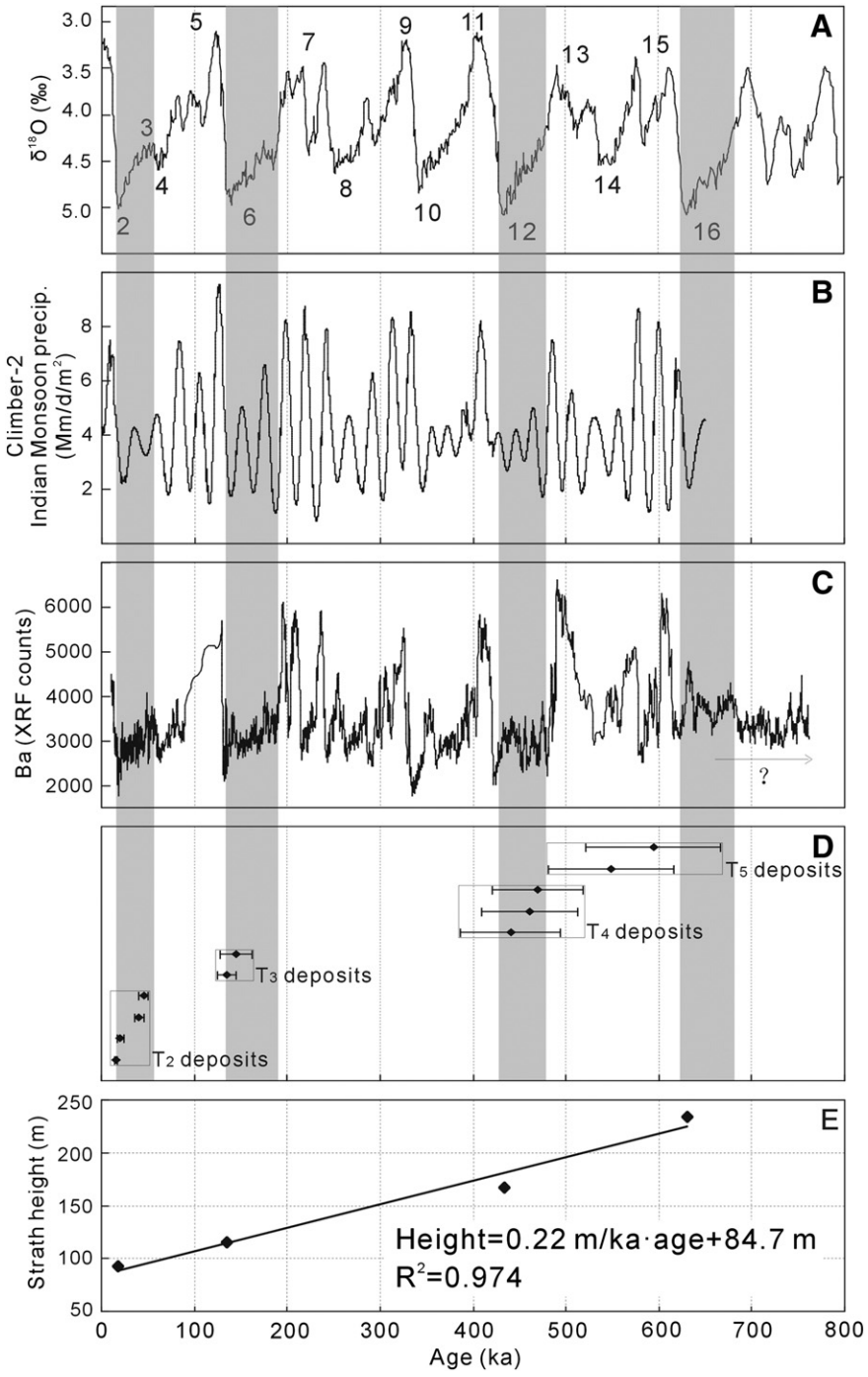

Figure 8. (A) LR04 benthic oxygen isotope stack (Lisiecki and Raymo, 2005). (B) CLIMBER-2 model-based Indian monsoon precipitation over the past 65 ka (Ziegler, 2009). (C) Barium counts (XRF-core scanning) from IMAGES Core MD04-2881, Murray Ridge, northeastern Arabian Sea (Ziegler et al., 2010). Ba is used here to be indicative of the intensity of the south Asian monsoon. The changes in Ba counts over the past 600 ka are consistent with modeled variations in the Indian monsoon precipitation as shown in Fig. 8 (B). (D) ESR ages of terraces T2–T5 deposits. (E) Reconstructed long-term bedrock incision rate (0.22 m/ka) over the past 630 ka according to the strath heights and ages of terraces T2–T5, lower reach of the Yazheku River.

https://doi.org/10.1016/j.yqres.2013.08.007 Published online by Cambridge University Press

both discharge volume and sediment flux in the Yazheku River were relatively low during glacial times.

At the beginning of the transition from glacial to interglacial climates, the glaciers in the Haizi Shan began to retreat in response to rising temperature. This would have caused a significant increase both in discharge and sediment supply, including clasts of all sizes. Meanwhile, permafrost began to melt, which would also have supplied much water and sediment to the Yazheku River. Additionally, the south Asian monsoon would have strengthened, leading to a rise in precipitation after solar insolation was enhanced (Fig. 8).

Continued climatic warming would have led to full interglacial conditions and glaciers in the Yazheku drainage basin would have melted away completely, after which fluvial discharge would have been supplied only by precipitation in the catchment. During this period, slopes would have been stabilized by colonizing vegetation and thus would have provided the Yazheku with quite limited amounts of sediment.

At the ends of interglacial periods, climate began to cool and, therefore, the south Asian monsoon would have started to weaken, which would have led to a decrease in precipitation (Fig. 8). Moreover, during this period, the cooling temperature, together with the reduced precipitation, would have caused the degradation of vegetation. Consequently, sediment flux into the Yazheku River increased. Thereafter, the climate returned to glacial conditions.

In summary, both discharge and sediment supply were relatively low in glacial periods, during which the two prerequisites mentioned above, i.e., the high sediment supplies (including boulders) and sufficient fluvial discharge for transporting them, could not be met. During interglacials the sediment flux was low (due to the vegetation growth), which is contrast to the large water volume resulting from the enhanced south Asian monsoon. This situation is more likely to have led to incision than to aggradation by the Yazheku. There might have been a phase of sediment accumulation during interglacial–glacial transitions, resulting from decreased precipitation and increased sediment supply. This potential aggradational phase, however, seems unlikely to have provided terraces T5–T2 with boulders up to several meters in diameter. It is reasonable to infer that the aggradation phases of boulders in terraces T5–T2 occurred during the glacial–interglacial transitions, when there were high sediment supplies (including different sized boulders) resulting from the melting of glaciers and permafrost, and enough water discharge also from the melting of glaciers and permafrost, as well as from the strengthened south Asian monsoon precipitation.

Timing of sediments of terraces T5–T2

For a strath terrace, the alluvium resting on the strath surface, especially if relatively thin (less than 3 m), is generally considered the carving tool that formed the strath and, therefore, the age of the alluvium is typically thought to be synchronous with that of the strath formation (Gilbert, 1877; Mackin, 1937; Bull, 1990; Merritts et al., 1994; Pazzaglia and Brandon, 2001; Wegmann and Pazzaglia, 2002). Aggradation of gravels on a strath surface, however, can also occur some time after the formation of the strath surface (e.g., Bull, 1990; Pazzaglia and Brandon, 2001). On the basis of ESR ages and the inference that the boulders in the T5–T2 gravel layers were deposited during glacial–interglacial transitions, we will present below a combination of the above two situations concerning the timing of sediment deposition on a strath surface, that is, aggradation of a terrace gravel unit was achieved by the above two different fluvial processes.

In order to better explain the timing of the T5–T2 deposits, we first select a typical terrace (i.e., T4) from T5–T2 to analyze. T4 has ESR ages of 440 ± 54 ka, 461 ± 52 ka, and 470 ± 49 ka, which can be assigned to MIS 12. According to the above inference (i.e., that emplacement of boulders in terraces T5–T2 occurred during glacial-interglacial transitions), the T4 gravel unit was probably deposited during the MIS 12–11 transition. The three dates, however, significantly pre-date the transition from MIS 12 to MIS 11. This probably means that the gravel layer of T4 was not the product of single fluvial aggradation, but represents two different depositional phases separated by a time interval. The basal part, where the ESR samples were collected and which probably served as the carving tool during the formation of the T4 strath, is likely to have been formed during the MIS 12 glacial expansion in the Haizi Shan. However, the upper part containing large boulders probably aggraded during the transition between MIS 12 and MIS 11, as a coupled consequence of (1) enhanced sediment supply from the melting of glaciers and permafrost in the Haizi Shan, and (2) increased water discharge from the glacier and permafrost melting, as well as from the strengthened monsoon precipitation then.

The basal part of the T3 gravel was dated to 135 ± 10 and 146 ± 17 ka, corresponding to late MIS 6. A strath is primarily created by bed gravel deposits through lateral erosion and valley-bottom widening. During this process, the channel would sweep laterally, carving the strath, and temporarily keeping alluvium in the floodplain. Progressive lateral sweeps of the channel would tend to remove previously deposited alluvium, leaving new and younger alluvium behind in its place. As a result, only a fragment of older alluvium, recording the onset and duration of strath cutting, would be preserved in the alluvium layer of a strath terrace (Wegmann and Pazzaglia, 2002). The above two ages (135 ± 10 ka and 146 ± 17 ka) probably indicate the timing immediately before the T4 strath was buried by the upper part of the T3 gravel unit (containing large boulders), which was probably formed during the melting phase of the MIS 6 glaciers in the Haizi Shan.

The T2 basal deposits have ESR ages of 16.4 ± 1.4 ka, 20.2 ± 3.5 ka, 40.4 ± 5.1 ka, and 45.3 ± 5.6 ka. The first two dates can be assigned to MIS 2, and the last two to MIS 3. It is worth noting that glacial advances during MIS 3 and MIS 2 have been widely identified in regions (including the Haizi Shan) that are climatically controlled by the south Asian monsoon (Owen et al., 2002, 2005; Xu and Zhou, 2009), and that the sampling locations of dates 40.4 ± 5.1 ka and 45.3 ± 5.6 ka are deeper than those of ages 16.4 ± 1.4 ka and 20.2 ± 3.5 ka. We infer that the basal part of the T2 gravels (with ESR ages of 40.4 ± 5.1 ka and 45.3 ± 5.6 ka) was deposited as the 'cutting tool' of the T2 strath during the Haizi Shan glacial advance in MIS 3, which was followed by the aggradation phase associated with the melting of glaciers and permafrost in the Haizi Shan during the later part of MIS 3 glacial expansion; erosion by the Yazheku River during the MIS 2 glacial advance removed most of the MIS 3 alluvium (but did not cut through the MIS 3 sediments into the bedrock) and, at the same time, left new, younger alluvium in its place; immediately after this was the accumulation phase (sediments with ages of 16.4 ± 1.4 ka and 20.2 ± 3.5 ka) related to the melting of glaciers and permafrost during the late LGM.

The basal part of the T5 gravel layer was dated to 549 ± 68 ka and 594 ± 73 ka, which can be assigned to MIS 15–13 and MIS 16–13 respectively, taking the age errors into account. Apparently, this assignment seems excessively uncertain, given that an aggradational phase typically lasts no more than thousands of years (e.g., Merritts et al., 1994). Here we follow the age model of the T5–T2 basal gravel units (i.e., they were deposited as strath cutting-tool 'lags' during glacial intervals) to estimate the corresponding marine isotope stages of ages 549 ± 68 ka and 594 ± 73 ka. There are two possibilities for the correlation between the ages and marine oxygen stages. Firstly, both of 549 ± 68 ka and 594 ± 73 ka are assigned to MIS 14. Secondly, 549 ± 68 ka is correlated to MIS 14, and 594 ± 73 ka to MIS 16. Both cases imply that the upper T5 gravels were likely deposited during the transition from MIS 14 to MIS 13, and that the large boulders contained in the T5 gravels were basically produced by glaciers in the Haizi Shan during MIS 14.

As suggested by the MIS curve in Figure 8A, the global ice volume during MIS 16 was even larger than in MIS 14, probably implying that, from a global view, the climatic condition in MIS 16 was more favorable for glacial development than during MIS 14. Moreover, on the basis of cosmogenic radionuclide ^{10}Be dating results, Wang et al. (2006) suggested an extensive glacial expansion during MIS 16 in the Haizi Shan. It is possible that the sample YZK05 (with age of 548.8 ± 67.6 ka) has

https://doi.org/10.1016/j.yqres.2013.08.007 Published online by Cambridge University Press

been reworked or partially bleached since its deposition and thus produced a younger age. Consequently, we infer that the basal part of the T5 sediments formed when glaciers in the Haizi Shan were advancing during MIS 16, and that the upper T5 gravels were deposited in the latter part of MIS 16. As discussed above, we cannot, however, rule out the possibility of a MIS 14 glaciation in the Haizi Shan and its contribution to the T5 gravel layer.

Incision of terraces T5–T2

Channel downcutting, which isolates the deposit that accumulated during the previous period and thus generates a terrace, occurs when stream power (consisting of those variables that if increased favor degradation; e.g., discharge, channel gradient) exceeds resisting power (composed of those variables that if increased favor aggradation; e.g., sediment flux) (cf. Bull, 1990, 1991). However, as discussed above ("Factors affecting the formation of Yazheku river terraces"), progressive incision, which leads to the formation of terrace staircases, cannot be achieved in response to climate alone. It can only occur in regions where the land surface is being uplifted (Maddy, 1997; Bridgland, 2000; Maddy et al., 2000; Westaway et al., 2002; Demir et al., 2004). The Haizi Shan has experienced several glaciations since the middle Pleistocene (Zheng and Ma, 1995; Li, 1996; Xu and Zhou, 2009). Ice caps up to hundreds of meters thick and with areas of several thousand square kilometers were formed on the Haizi Shan during the Quaternary glaciations (Zheng and Ma, 1995; Li, 1996). The loading of these huge ice caps would have restrained or dampened the uplift behavior, or even have caused crustal subsidence (Sigvaldason et al., 1992; Motyka, 2003). In contrast, during the glacial–interglacial transitions, the glaciers on the Haizi Shan would have retreated in response to the rising temperature. As the volume of the glaciers decreased to the critical value, the unloading resulting from the glacier melting would have caused isostatic crustal rebound, during which the energy for tectonic activity accumulated during the former glacial expansion would have been released (Andrews, 1968; Sigvaldason et al., 1992; Brevik and Reid, 2000; Maddy and Bridgland, 2000; Motyka, 2003; Bridgland et al., 2010). As a result, rapid uplift would have occurred in the Haizi Shan region. This rapid uplift would have significantly enhanced the stream power of the Yazheku and thus led to the downcutting and consequent terrace formation. The incision process would probably have continued until the end of the following interglacial, when the sediment supply increased and fluvial discharge decreased (see section "Boulders in the sediments of terraces T5–T2"). Based on the discussions in "Timing of sediments of terraces T5–T2" above, we infer that the downcutting events that caused the formation of T5–T2 terraces probably occurred during the transitions of MIS 16–15, MIS 12–11, MIS 6–5, and MIS 2–1.

The Yazheku terraces can be correlated with those in the surrounding regions. For example, the fifth terrace in the Shuoqu River, a second-order tributary of the Yangtze about 100 km southwest of the Yazheku, was dated to 504.5 ± 50.5 ka by Xu and Zhou (2007). Yang et al. (2003) recognized four terraces along the Minjiang River, at the eastern margin of the Tibetan Plateau, and they dated the third terrace to ~460 ka. Li et al. (2001) dated a series of terraces (seven levels in total) in the Three Gorges, middle reach of the Yangtze River. Among these the fourth terrace has an age of ~490 ka. The approximate timing of these terraces probably suggests that the downcuttings, which led to their formation, were controlled by a same forcing, climate change. Possibly because of optimal preservation as landforms, and being amenable to a variety of dating methods (especially ^{14}C dating), terraces with similar ages to T2 have been widely recognized in the eastern Tibetan Plateau (Zhou et al., 1996; Li et al., 2001; Wen et al., 2003; Yang et al., 2003; Xu and Zhou, 2007). This supports the above inference.

A long-term bedrock incision rate for the Yazheku River has been established based on the heights of the T5–T2 strath surfaces above the modern river level and the times when the straths were incised. As presented above, the straths were formed during glacial expansions of the Haizi Shan, and then were covered by alluvial deposits from the melting of glaciers and permafrost during glacial–interglacial transitions, finally being isolated by downcutting when stream power exceeded resistance to erosion. We have obtained the ages of the basal parts of the T5–T2 gravel units. The ages are probably indicative of the formation times of the T5–T2 straths, but not the timing of the vertical incision events. In any case, we can roughly assign the T5–T2 downcutting events to the transitions of 16–15, MIS 12–11, MIS 6–5, and MIS 2–1, respectively. The estimated bedrock incision rate since 620 ka is ~0.22 mm/yr (Fig. 8), which is comparable to other regions in the Tibetan Plateau. The Yezigou River in the eastern Qilian Mountains, eastern Tibetan Plateau, has an average incision rate of 0.25 mm/yr since MIS 12 (Pan et al., 2007). The long-term bedrock incision rate of the Shagou River, another river in the eastern Qilian Mountains, is 0.14 mm/yr, which has been nearly steady for the past 850 ka (Pan et al., 2003). The bedrock incision rate of the Yazheku River has varied significantly over different time periods. Its incision rate between MIS 12 and MIS 6 is averaged to 0.17 mm/yr, which is slightly lower than that during MIS 6–MIS 2 (0.19 mm/yr), and dramatically lower than that during MIS 16–MIS 12 (0.34 mm/yr). The much higher incision rate during MIS 16–MIS 12 is probably related to the more intensive tectonic activity in this period as indicated by the Kunlun–Huanghe Movement.

Strath formation of terraces T5–T2

Erosional widening of valley floors primarily occurs when a river incises downward and laterally, generally into bedrock (sometimes into the sediments of a previously formed terrace, thus the formation of a fill-cut terrace like T2a/T2b/T2c of the Yazheku River) to form a broad flat valley bottom (i.e., strath) (Pazzaglia and Brandon, 2001). This process of strath formation commonly occurs during periods of equilibrium (Bull, 1990, 1991). As discussed above, aggradation dominated the transitions from and to glacial periods, and downcutting prevailed from the end of glacial–interglacial transitions to the later parts of interglacials. From this we infer that the straths of terraces T5–T2 were created sometime during glacial periods. Ages of basal parts of T5–T2 sediments support this inference (section "Timing of sediments of terraces T5–T2" and Fig. 8). Specifically, the timing of the formation of the T5–T2 straths can be assigned to MIS 16, 12, 6, and 3, respectively.

Summary

The Yazheku River, flowing down a former glacial valley from the Haizi Shan, which was greatly uplifted and repeatedly glaciated during the Quaternary, has formed five major terraces (T5, T4, T3, T2, and T1, in order of decreasing age) and three small-scale fill-and-cut terraces (T2c, T2b, and T2a). Geomorphic and sedimentological investigations and ESR dating were carried out to understand the formation processes and associated forcings of the four higher strath terraces (T5, T4, T3, and T2). At least four driving factors, climate change, tectonic uplift, regional (epeirogenic) uplift, and paleo-glacier activity, have influenced the generation of the four terraces. The straths of terraces T5–T2 were created during the Haizi Shan glacial expansions in MIS16, 12, 6, and 4–3, respectively, when the lower reach of the Yazheku River was in equilibrium, with no significant aggradation or downcutting. Each of the T5–T2 gravel units can be divided into two portions based on their sedimentary features such as grain size. The basal parts were deposited as strath cutting-tool gravels when glaciers in the Haizi Shan advanced during MIS 16, 12, 6, and 4–3. In contrast, the upper portions, containing numerous decimeter to meter-sized boulders, represent major aggradation phases of the T5–T2 terraces and were deposited during the MIS 16, 12, 6, and 2 deglaciations respectively, when sediment supply was greatly increased by the melting of ice and permafrost in the Haizi Shan. The vertical incisions, which led to the generation of the four terraces, immediately followed the main aggradation phases of the T5–T2 gravel units. Specifically, the incisions occurred during the transitions of

https://doi.org/10.1016/j.yqres.2013.08.007 Published online by Cambridge University Press

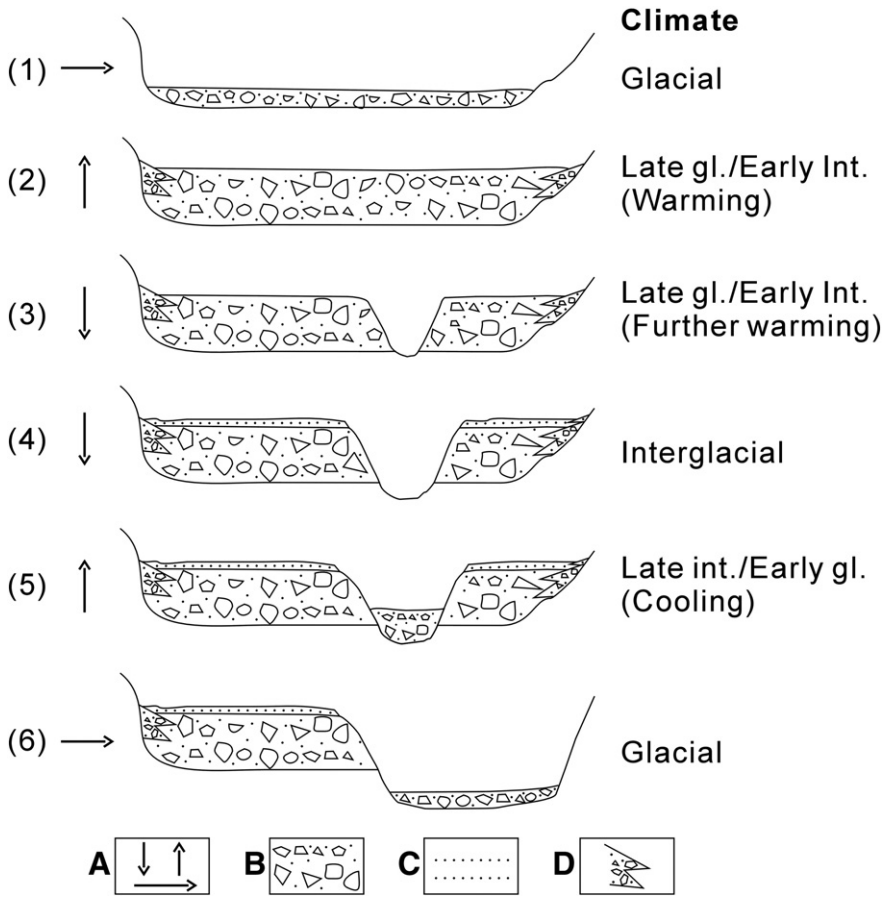

Figure 9. A model of strath terrace formation in the lower reach of the Yazheku River, which was affected by climate change, glaciation, tectonic activity, and glacial isostatic rebound as well. In this model, the formation process of a strath terrace can be decomposed into the following six phases: (1) strath formation during glacial periods, when the lower reach of the Yazheku River was in equilibrium state, with no significantly aggradation or downcutting; (2) main aggradation phase (including the deposition of large granite boulders) occurring when the glaciers and permafrost in the Haizi Shan began to melt during the transition from glacial to interglacial climates; (3) vertical incision happening when the volume of the glaciers in the Haizi Shan reduced to the critical value, which would have caused isostatic crustal rebound and consequently the enhanced stream power; (4) continued incision during full interglacial periods as a consequence of the increased precipitation (resulting from the strengthened south Asian monsoon) and reduced sediment supply (due to the colonized vegetation); (5) an aggradation phase during the interglacial–glacial transitions, when the vegetation began to degrade and led to a rise in sediment supply and, meanwhile, the precipitation started to decrease due to the weakened south Asian monsoon; and (6) return to phase (1). A: direction of erosion or aggradation; B: alluvia; C: flood plain deposits; D: solifluction and slope-wash deposits.

MIS 16–15, MIS 12–11, MIS 6–5, and MIS 2–1. During the downcutting phases, fluvial discharge prevailed over sediment flux and, moreover, the Haizi Shan was elevated simultaneously by glacio-isostatic rebound. Finally, the above formation process of the Yazheku strath terraces is summarized in a model depicted in Figure 9.

Acknowledgments

We thank Yuguang Ye and Shaobo Diao for their assistance in the ESR dating. We thank David R. Bridgland and an anonymous reviewer for their constructive and helpful comments and suggestions. We also thank the editor, Alan Gillespie, for his careful editorial work and his encouragement to us. This work was supported by the National Natural Science Foundation of China (no. 41271077), "Strategic Priority Research Program (B)" of the Chinese Academy of Sciences (grant no. XDB03030100), and Guangdong Natural Science Foundation (no. S2012010008610).

References

Adamiec, G., Aitken, M.J., 1998. Dose-rate conversion factors: update. Ancient TL 16, 37–50.
Andrews, J.T., 1968. Pattern and cause of variability of postglacial uplift and rate of uplift in Arctic Canada. J. Geol. 76, 404–425.
Brevik, E.C., Reid, J.R., 2000. Uplift-based limits to the thickness of ice in the Lake Agassiz basin of North Dakota during the Late Wisconsinan. Geomorphology 32, 161–169.
Bridgland, D.R., 2000. River terrace systems in north-west Europe: an archive of environmental change, uplift and early human occupation. Quat. Sci. Rev. 19, 1293–1303.
Bridgland, D.R., Westaway, R., Howard, A.J., Innes, J.B., Long, A.J., Mitchell, W.A., White, M.J., White, T.S., 2010. The role of glacio-isostasy in the formation of post-glacial river terraces in relation to the MIS 2 ice limit: evidence from northern England. Proc. Geol. Assoc. 121, 113–127.
Bull, W.B., 1990. Stream-terrace genesis: implications for soil development. Geomorphology 3, 351–367.
Bull, W.B., 1991. Geomorphic response to climatic change. Oxford University Press, New York 12–34.
Cui, Z., Wu, Y., Liu, G., 1997. Discovery of the "Kunlun–Huanghe Movement". Chin. Sci. Bull. 42, 1986–1989.
Cui, Z., Wu, Y., Liu, G., 1998. On the "Kunlun–Huanghe Movement". Sci. China (Ser. D) 28, 53–59.
Cunha, P.P., Martins, A.A., Daveau, S., Friend, P.E., 2005. Tectonic control of the Tejo River fluvial incision during the late Cenozoic, in Ródão-central Portugal (Atlantic Iberian border). Geomorphology 64, 271–298.
Demir, T., Yesilnacar, I., Westaway, R., 2004. River terrace sequences in Turkey: sources of evidence for lateral variations in regional uplift. Proc. Geol. Assoc. 115, 289–311.
Fisk, H.N., 1951. Loess and Quaternary geology of the Lower Mississippi Valley. J. Geol. 59, 333–356.
Gilbert, G.K., 1877. Geology of the Henry Mountains (Utah). Geographical and Geological Survey of the Rocky Mountains Region. U.S. Government Printing Office, Washington D.C. (170 pp.).
Grün, R., 1989. Electron spin resonance (ESR) dating. Quat. Int. 1, 65–109.
Hou, Z., Qu, X., Zhou, J., 2001. Collision-orogenic processes of the Yidun Arc in the Sanjiang region: records of granites. Acta Geol. Sin. 75 (4), 484–497 (In Chinese with English abstract).
Hou, Z., Yang, Y., Qu, X., 2004. Tectonic evolution and mineralization systems of the Yidun Arc orogen in the Sanjiang region, China. Acta Geol. Sin. 78 (1), 109–120 (In Chinese with English abstract).

https://doi.org/10.1016/j.yqres.2013.08.007 Published online by Cambridge University Press

Hsieh, M.L., Knuepfer, P.L.K., 2001. Middle-late Holocene river terraces in the Erhien River Basin, southwestern Taiwan—implications of river response to climate change and active tectonic uplift. Geomorphology 38, 337–372.
Jin, S.Z., Deng, Z., Huang, P.H., 1991. Study on optical effects of quartz E' center in loess. Chin. Sci. Bull. 36, 1865–1870.
Laurent, M., Falgueres, C., Bahain, J.J., Rousseau, L., Lanoe, V.V., 1998. ESR dating of quartz extracted from Quaternary and Neogen sediments: method potential and actual limits. Quat. Geochronol. 17, 1057–1062.
Li, J., 1996. Glaciers in the Hengduan Mountains. Science Press, Beijing (In Chinese with English abstract).
Li, J., Fang, X., 1998. Uplift of the Tibetan Plateau and paleo-environmental changes. Chin. Sci. Bull. 43 (15), 1569–1574.
Li, J., Fang, X., Ma, H., 1996. Landform evolution of the upper Huanghe River and uplift of the Tibetan Plateau in the Late Cenozoic. Sci. China (Ser. D) 26, 316–322.
Li, J., Xie, S., Kuang, M., 2001. Geomorphic evolution of the Yangtze Gorges and the time of their formation. Geomorphology 41, 125–135.
Lin, Z., Wu, X., 1990. A study on the path of moisture transportation in the Tibetan Plateau. Geogr. Res. 9, 33–39 (In Chinese with English abstract).
Lisiecki, L.E., Raymo, M.E., 2005. A Pliocene–Pleistocene stack of 57 globally distributed benthic δ18O records. Paleoceanography 20 (PA1003).
Litchfield, N.J., Berryman, K.R., 2005. Correlation of fluvial terraces within the Hikurangi Margin, New Zealand: implications for climate and baselevel controls. Geomorphology 68, 291–313.
Mackin, J.H., 1937. Erosional history of the Big Horn basin, Wyoming. Geol. Soc. Am. Bull. 48, 813–893.
Maddy, D., 1997. Uplift driven valley incision and River Terrace formation in Southern England. J. Quat. Sci. 12, 539–545.
Maddy, D., Bridgland, D.R., 2000. Accelerated uplift resulting from Anglian glacioisotatic rebound in the Middle Thames Valley, UK?: evidence from the river terrace record. Quat. Sci. Rev. 19, 1581–1588.
Maddy, D., Bridgland, D.R., Green, C.P., 2000. Crustal uplift in southern England: evidence from the river terrace records. Geomorphology 33, 167–181.
Maddy, D., Bridglandm, D., Westawaym, R., 2001. Uplift-driven valley incision and climate-controlled river terrace development in the Thames Valley, UK. Quat. Int. 79, 23–36.
Mejdahl, V., 1979. Thermoluminescence dating: beta-dose attenuation in quartz grains. Archaeometry 21, 61–72.
Merritts, D.J., Vincent, K.R., Wohl, E.E., 1994. Long river profiles, tectonism, and eustasy: a guide to interpreting fluvial terraces. J. Geophys. Res. 99 (B7), 14031–14050.
Motyka, R.J., 2003. Little Ice Age subsidence and post Little Ice Age uplift at Juneau, Alaska, inferred from dendrochronology and geomorphology. Quat. Res. 59, 300–309.
Owen, L.A., Finkel, R.C., Caffee, M.W., 2002. A note on the extent of glaciation throughout the Himalayan during the global Last Glacial Maximum. Quat. Sci. Rev. 21, 147–157.
Owen, L.A., Finkel, R.C., Barnard, P.L., Haizhou, M., Asahi, K., Caffee, M.W., Derbyshire, E., 2005. Climatic and topographic controls on the style and timing of Late Quaternary glaciation throughout Tibet and the Himalaya defined by ^{10}Be cosmogenic radionuclide surface exposure dating. Quat. Sci. Rev. 24, 1391–1411.
Pan, B., Burbank, D., Wang, Y., Wu, G., Li, J., Guan, Q., 2003. A 900 ky record of strath terrace formation during glacial–interglacial transitions in northwest China. Geology 31 (11), 957–960.
Pan, B., Gao, H., Wu, G., Li, J., Li, B., Ye, Y., 2007. Dating of erosion surface and terraces in the eastern Qilian Shan, northwest China. Earth Surf. Process. Landforms 32, 143–154.
Pazzaglia, F.J., Brandon, M.T., 2001. A fluvial record of long-term steady-state uplift and erosion across the Cascadia forearc high, western Washington State. Am. J. Sci. 30, 385–431.
Penck, A., Brückner, E., 1909. Die alpen im Eiszeitalter. Tauchnitz, Leipzig 1199.
Prescott, J.R., Hutton, J.T., 1994. Cosmic ray contributions to dose rates for luminescence and ESR dating: large depths and long-term time variations. Radiat. Meas. 23, 497–500.
Prescott, J.R., Robertson, G.B., 1997. Sediment dating by luminescence: a review. Radiat. Meas. 27, 893–922.
Rick, W.J., 1997. Electron spin resonance (ESR) dating and ESR applications in Quaternary science and archaeometry. Radiat. Meas. 27, 975–1025.
Schwarcz, H.P., 1994. Current challenges to ESR dating. Quat. Sci. Rev. 13, 601–605.
Shi, Y., 2002. Characteristics of late Quaternary monsoonal glaciation on the Tibetan Plateau and in East Asia. Quaternary International 79–91 (97/98).
Shi, Y., 2006. The Quaternary glaciations and environmental variations in China. Hebei Science and Technology Publishing, Shijiazhuang (In Chinese with English abstract).
Shi, Y., Zheng, B., Li, S., Ye, B., 1995. Studies on altitude and climatic environment in the middle and eastern parts of the Tibetan Plateau during Quaternary maximum glaciation. J. Glaciol. Geocryol. 17, 97112.
Sigvaldason, G.E., Annertz, K., Nilsson, M., 1992. Effect of glacier loading/deloading on volcanism: postglacial volcanic production rate of the Dyngjufjiill area, central Iceland. Bull. Volcanol. 54, 385–392.
Starkel, L., 2003. Climatically controlled terraces in uplifting mountain areas. Quat. Sci. Rev. 22, 2189–2198.
Toyoda, S., Voinchet, P., Falguères, C., Dolo, J.M., Laurent, M., 2000. Bleaching of ESR signals by the sunlight: a laboratory experiment for establishing the ESR dating of sediments. Appl. Radiat. Isot. 52, 1357–1362.
Vandenberghe, J., 2003. Climate forcing of fluvial system development: an evolution of ideas. Quat. Sci. Rev. 22, 2053–2060.
Walther, R., Zilles, D., 1994. ESR studies on bleached sedimentary quartz. Quat. Sci. Rev. 13, 611–614.
Wang, J., Raisbeck, R., Xu, X., Yiou, F., Bai, S., 2006. In situ cosmogenic ^{10}Be dating of the Quaternary glaciations in the southern Shaluli Mountain on the Southeastern Tibetan Plateau. Sci. China (Ser. D) 49, 1291–1298.
Watchman, A.L., Twidale, C.R., 2002. Relative and 'absolute' dating of land surfaces. Earth Sci. Rev. 58, 1–49.
Wegmann, K.W., Pazzaglia, F.J., 2002. Holocene strath terraces, climate change, and active tectonics: the Clearwater River basin, Olympic Peninsula, Washington State. Geol. Soc. Am. Bull. 114 (6), 731–744.
Wen, X., Xu, X., Zheng, R., Xie, Y., Wan, C., 2003. Average slip rate and earthquake rupturing of the Ganzi–Yushu fault zone. Sci. China (Ser. D) 33, 199–208.
Westaway, R., Maddy, D., Bridgland, D.R., 2002. Flow in the lower continental crust as a mechanism for the Quaternary uplift of southeast England: constraints from the Thames terrace record. Quat. Sci. Rev. 21, 559–603.
Xu, L., Zhou, S., 2007. River Terraces in the Shuoqu River and their response to mountain uplift and climate changes in Western Sichuan Province. J. Glaciol. Geocryol. 4, 603–612.
Xu, L., Zhou, S., 2009. Quaternary glaciations recorded by glacial and fluvial landforms in the Shaluli Mountains, southeastern Tibetan Plateau. Geomorphology 103, 268–275.
Xu, X., Wen, X., Yu, G., Zheng, R., Luo, H., Zheng, B., 2005. Average slip rate, earthquake rupturing segmentation and recurrence behavior on the Litang fault zone, western Sichuan Province, China. Sci. China (Ser. D: Earth Sci.) 48, 1183–1196.
Yang, N., Zhang, Y., Meng, H., Zhang, H., 2003. Terraces in the Minjiang River, western Sichuan Plateau. J. Geomech. 9, 363–370.
Zeuner, F.E., 1945. The Pleistocene Period: its Climate, Chronology and Faunal Successions, 1st ed. Royal Society, Publication No. 130, London 322.
Zhang, Q., Zhou, Y., Lu, X., Xu, Q., 1990. Uplifting rate of the modern Tibetan Plateau. Chin. Sci. Bull. 35 (7), 529–531.
Zheng, B., Ma, Q., 1995. A study on the geomorphological characteristics and glaciations in Paleo-Daocheng Ice Cap, western Sichuan. J. Glaciol. Geocryol. 17, 23–32 (In Chinese with English abstract).
Zheng, X., Xu, J., Li, X., 1997. Characteristics of water vapour transfer in upper troposphere over the Tibetan Plateau. Plateau Meteorol. 16, 274–281 (In Chinese with English abstract).
Zhao, J, Song, Y, King, J.W., Liu, S, Wang, J, Wu, M, 2010. Glacial geomorphology and glacial history of the Muzart River valley, Tianshan range, China. Quat. Sci. Rev. 29, 1453–1463.
Zhao, J, Zhou, S, He, Y, Ye, Y, Liu, S, 2006. ESR dating of glacial tills and glaciations in the Urumqi River headwaters, Tianshan Mountains, China. Quat. Int. 144, 61–67.
Zhou, R., Ma, S., Cai, C., 1996. Late Quaternary active features of the Ganzi–Yushu fault zone. Earthq.Res. China 12, 250–260.
Zhuo, G., Xu, X., Chen, L., 2002. Water distribution feature of summer precipitation on the Tibetan Plateau. Sci. Meteorol. Sin. 22, 1–8 (In Chinese with English abstract).
Ziegler, M., 2009. Orbital forcing of the late Pleistocene boreal summer monsoon: links to North Atlantic cold events and the El Niño–Southern Oscillation. Geol. Ultraiect. 313, 141.
Ziegler, M., Lourens, L.J., Tuenter, E., Reichart, G.-J., 2010. High Arabian Sea productivity conditions during MIS 13 — odd monsoon event or intensified overturning circulation at the end of the Mid-Pleistocene transition? Clim. Past 6, 63–76.

https://doi.org/10.1016/j.yqres.2013.08.007 Published online by Cambridge University Press